Journal of Sound and Vibration (2001) **241**(5), 839–855
doi:10.1006/jsvi.2000.3330, available online at http://www.idealibrary.com on IDEAL®

A MESH-FREE METHOD FOR STATIC AND FREE VIBRATION ANALYSES OF THIN PLATES OF COMPLICATED SHAPE

G. R. Liu and X. L. Chen

Centre for Advanced Computations in Engineering Science, c/o: Department of Mechanical Engineering, The National University of Singapore, 10 Kent Ridge Crescent, Singapore 119260, *Singapore. E-mail: mpeliugr@nus.edu.sg*

(*Received* 26 *January* 2000, *and in final form* 12 *September* 2000)

A mesh-free method is presented to analyze the static deflection and the natural frequencies of thin plates of complicated shape. The present method uses moving least-squares (MLS) interpolation to construct shape functions based on a set of nodes arbitrarily distributed in the analysis domain. Discrete system equations are derived from the variational form of system equation. For static analysis, a penalty method is presented to enforce the essential boundary conditions. For frequency analysis of free vibration, the essential boundary conditions are represented through a weak form and imposed using orthogonal transformation techniques. The present EFG method together with techniques for imposing boundary conditions is coded in Fortran. Numerical examples are presented for rectangular, elliptical, polygonal and complicated plates to demonstrate the convergence and efficiency of the present method.

1. INTRODUCTION

With the wide application of plate structures of complex geometry, static and dynamic analyses of plates of complicated shape become very important. However, exact analyses of such a plate are usually very difficult. Therefore, numerical techniques with different discretization schemes such as finite element method (FEM) have been developed. FEM has achieved remarkable success in the static and dynamic analyses of plates. However, in the FEM as mesh is required to establish element connectivity to form finite element equations.

In recent years, a new type of numerical method called mesh-free method (MFM) is being developed in the area of computational mechanics. Different versions of MFMs [1–3] have been so far successfully formulated for stress and displacement analysis in solids (e.g., references [4–8]), fluid flow analysis (e.g., references [9, 10]), and heat transfer simulation [11]. All the MFM formulations use a set of nodes scattered in the problem domain, and do not require any element connectivity among the nodes. Element free Galerkin (EFG) method is a well-developed method which uses moving least square (MLS) approach for displacement interpolation. The EFG method has been applied to elasticity [12], crack growth [13], and many other problems. Krysl and Belytschko have extended the EFG method to static analysis of thin plates and shells [14, 15]. In their work, the essential boundary conditions are enforced by a method of Lagrange multipliers. An EFG method has also been formulated for modal analyses of Euler–Bernoulli beams and Kirchhoff plates [16]. In this work, the essential boundary conditions are enforced directly at each

0022-460X/01/150839 + 17 $35.00/0

constraint boundary point, and analysis of thin plates with straight lines have been performed.

In EFG methods, MLS interpolation functions are not equal to unity at nodes, which implies that the shape functions do not have the delta function property. This complicates the imposition of essential boundary conditions. Some techniques have been proposed to impose essential boundary conditions such as Lagrange multipliers [1], penalty method [17], coupling with FEM [18], and coupling with boundary element method (BEM) [19, 20].

Use of Lagrange multipliers in the EFG methods leads to an increase of unknowns in the discrete algebraic system equation and zero diagonal terms in the stiffness matrix. Therefore, solving the discrete system equations becomes more complex and less efficient. In the present paper, for static deflection of thin plates, an EFG method is presented utilizing penalty approach to enforce essential boundary conditions. The discrete system equation so derived has a simple form as that contained in the conventional FEM. For the analysis of free vibration of thin plates, the essential boundary conditions are formulated through a weak form, which is separated from the weak form for the system equation. The boundary conditions are then imposed using orthogonal transform techniques. The eigenvalue equation derived using the present approach possesses a much smaller dimension than the one in FEM. A number of numerical examples have been presented. Static deflections of thin rectangular plates with fully clamped and simply supported boundaries are computed using the present approach. Natural frequencies of thin square, elliptical, hexagonal and complicated plates with different boundaries such as free, simply supported and fully clamped are also calculated. Both regularly and irregularly distributed nodes are used in the computation. Very good convergence and agreements are achieved compared to analytical solutions. The effectiveness of the present EFG method has been demonstrated through the examples for both static and free vibration analyses of complicated plates.

2. APPROXIMATION OF DISPLACEMENT

2.1. SHAPE FUNCTION

Consider a Kirchhoff plate of $a \times b \times h$ shown in Figure 1. A Cartesian co-ordinate system is used to establish equations. The deflections of the plate in the x, y, z directions are denoted as u, v, w respectively.

Based on Kirchhoff's assumption of thin plate, the deflection $w(\mathbf{X})$ at $\mathbf{X} = \{x, y\}^{\mathrm{T}}$ can be taken as an independent variable, and the other two displacements $u(\mathbf{X})$ and $v(\mathbf{X})$ can be

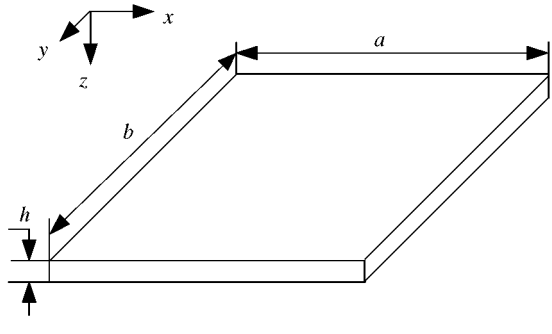

Figure 1. A thin rectangular plate and its co-ordinate system.

obtained through $w(\mathbf{X})$. In this paper, the moving least-squares (MLS) approximation is employed to approximate $w(\mathbf{X})$ with a displacement approximation function $w^h(\mathbf{X})$ given in the form of

$$w^h(\mathbf{X}) = \mathbf{P}^{\mathrm{T}}(\mathbf{X})\mathbf{a}(\mathbf{X}), \tag{1}$$

where $\mathbf{P}(\mathbf{X})$ is a complete polynomial of order m. The polynomials adopted in the present paper are

$$\mathbf{P}^{\mathrm{T}}(\mathbf{X}) = \{1, x, y, x^2, xy, y^2\}, \quad m = 6. \tag{2}$$

The coefficients $\mathbf{a}(\mathbf{X})$ in equation (1) are also functions of $\mathbf{X}$, which can be obtained by minimizing a weighted discrete L_2 norm:

$$\mathbf{J} = \sum_{I=1}^{n} w(\mathbf{X} - \mathbf{X}_I)[\mathbf{P}^{\mathrm{T}}(\mathbf{X}_I)a(\mathbf{X}) - w_I]^2, \tag{3}$$

where n is the number of points in the neighborhood of $\mathbf{X}$. The neighborhood is called the domain of influence of $\mathbf{X}$. $w(\mathbf{X} - \mathbf{X}_I)$ is a weight function of compact support.

$\partial J/\partial \mathbf{a} = 0$ yields the following linear algebraic equations:

$$\mathbf{A}(\mathbf{X})\mathbf{a}(\mathbf{X}) = \mathbf{B}(\mathbf{X})\mathbf{w}, \tag{4}$$

where $\mathbf{w} = \{w_1, \ldots, w_n\}^{\mathrm{T}}$, the symmetrical matrix $\mathbf{A}(\mathbf{X})$ and the non-symmetrical matrix $\mathbf{B}(\mathbf{X})$ are defined by the following forms:

$$\mathbf{A}(\mathbf{X}) = \sum_{I=1}^{n} w(\mathbf{X} - \mathbf{X}_I)\mathbf{P}(\mathbf{X}_I)\mathbf{P}^{\mathrm{T}}(\mathbf{X}_I), \tag{5}$$

$$\mathbf{B}(\mathbf{X}) = \{w(\mathbf{X} - \mathbf{X}_1)\mathbf{P}(\mathbf{X}_1), \ldots, w(\mathbf{X} - \mathbf{X}_n)\mathbf{P}(\mathbf{X}_n)\}. \tag{6}$$

Substituting equation (4) into equation (1), yields

$$w^h(\mathbf{X}) = \sum_{I=1}^{n} \mathbf{P}^{\mathrm{T}}(\mathbf{X})\mathbf{A}^{-1}(\mathbf{X})\mathbf{B}(\mathbf{X})w_I = \sum_{I=1}^{n} \Phi_I(\mathbf{X})w_I. \tag{7}$$

Let $\gamma(\mathbf{X}) = \mathbf{A}^{-1}(\mathbf{X})\mathbf{P}(\mathbf{X})$, we have

$$\Phi_I(\mathbf{X}) = \gamma^{\mathrm{T}}(\mathbf{X})\mathbf{B}(\mathbf{X}), \qquad \mathbf{A}\gamma = \mathbf{P}. \tag{8, 9}$$

The partial derivatives of γ can be obtained as follows:

$$\mathbf{A}\gamma_{,x} = \mathbf{P}_{,x} - \mathbf{A}_{,x}\gamma, \quad \mathbf{A}\gamma_{,y} = \mathbf{P}_{,y} - \mathbf{A}_{,y}\gamma, \tag{10, 11}$$

$$\mathbf{A}\gamma_{,xx} = \mathbf{P}_{,xx} - (\mathbf{A}_{,xx}\gamma + 2\mathbf{A}_{,x}\gamma_{,x}), \tag{12}$$

$$\mathbf{A}\gamma_{,xy} = \mathbf{P}_{,xy} - (\mathbf{A}_{,xy}\gamma + \mathbf{A}_{,x}\gamma_{,y} + \mathbf{A}_{,y}\gamma_{,x}), \tag{13}$$

$$\mathbf{A}\gamma_{,yy} = \mathbf{P}_{,yy} - (\mathbf{A}_{,yy}\gamma + 2\mathbf{A}_{,y}\gamma_{,y}). \tag{14}$$

The partial derivatives of shape function Φ_I can be obtained as follows:

$$\Phi_{I,x} = \gamma_{,x}^{\mathrm{T}}\mathbf{B}_I + \gamma^{\mathrm{T}}\mathbf{B}_{I,x}, \quad \Phi_{I,y} = \gamma_{,y}^{\mathrm{T}}\mathbf{B}_I + \gamma^{\mathrm{T}}\mathbf{B}_{I,y}, \tag{15, 16}$$

$$\Phi_{I,xx} = \gamma_{,xx}^{\mathrm{T}}\mathbf{B}_I + 2\gamma_{,x}^{\mathrm{T}}\mathbf{B}_{I,x} + \gamma^{\mathrm{T}}\mathbf{B}_{I,xx}, \tag{17}$$

$$\Phi_{I,xy} = \gamma_{,xy}^{\mathrm{T}}\mathbf{B}_I + \gamma_{,x}^{\mathrm{T}}\mathbf{B}_{I,y} + \gamma_{,y}^{\mathrm{T}}\mathbf{B}_{I,x} + \gamma^{\mathrm{T}}\mathbf{B}_{I,xy}, \tag{18}$$

$$\Phi_{I,yy} = \gamma_{,yy}^{\mathrm{T}}\mathbf{B}_I + 2\gamma_{,y}^{\mathrm{T}}\mathbf{B}_{I,y} + \gamma^{\mathrm{T}}\mathbf{B}_{I,yy}. \tag{19}$$

2.2. WEIGHT FUNCTION

The domains of influence of EFG nodes can be controlled by choosing a weight function. The choice of weight function is therefore very important. In addition, numerical integration to be produced by a weak form of equilibrium equation is performed at each Gauss point over background integration mesh. So the choice of both the size of background mesh and the number of Gauss points, is also important [21]. In this paper, the weight function for Kirchhoff plate is chosen as the quartic spline due to the requirement of the continuity of the weight function and its first and second order derivatives. The spline can be written as a function of a normalized distance:

$$w(r) = \begin{cases} (1 - 6r^2 + 8r^3 - 3r^4) & \text{for } 0 \leqslant r \leqslant 1, \\ 0 & \text{for } r > 1. \end{cases} \tag{20}$$

The choice of the shape of this influence domain is arbitrary. In most cases, square domains and circular domains are used. In this paper, square domains are used.

The weight function of square domains is written as

$$w(\mathbf{r}) = w(r_x)w(r_y) = w_x w_y, \tag{21}$$

$$r_x = \frac{\|x - x_I\|}{d_{mx}}, \qquad r_y = \frac{\|y - y_I\|}{d_{my}}, \tag{22, 23}$$

where $d_{mx} = d_{max}c_{xI}$, $d_{my} = d_{max}c_{yI}$, while d_{max} is a scaling parameter. c_{xI} and c_{yI} are determined to ensure that enough neighbor EFG nodes are included to produce a non-singular matrix $\mathbf{A}$.

3. GOVERNING EQUATIONS

The boundary conditions of a plate can be denoted as follows:

$$\sigma \cdot \mathbf{n} = \bar{\mathbf{t}} \quad \text{on } S_\sigma, \quad \tilde{\mathbf{u}} = \bar{\mathbf{u}} \quad \text{on } S_u, \tag{24, 25}$$

where $\tilde{\mathbf{u}} = \mathbf{R}w$.

For clamped boundary, $\mathbf{R} = \begin{Bmatrix} 1 \\ \dfrac{\partial}{\partial n} \end{Bmatrix}$.

For simply supported boundary, $\mathbf{R} = \begin{Bmatrix} 1 \\ \dfrac{\partial^2}{\partial n^2} \end{Bmatrix}$,

where σ is the stress tensor, $\mathbf{n}$ is the unit normal on the boundary of the domain V, and $\bar{\mathbf{t}}$ and $\bar{\mathbf{u}}$ denote prescribed boundary forces and displacements respectively.

Because the Kronecker delta condition $\mathbf{\Phi}_I(x_J) = \delta_{IJ}$ at each node is not satisfied by the MLS shape function, the essential boundary conditions (25) need to be imposed in a proper manner.

For static deflection analysis of thin plates, we use penalty method to enforce essential boundary conditions by adding an additional boundary condition term in the variational form of the static elastic equilibrium equation. The modified variational form can be written as

$$\int_S \delta\varepsilon_p^{\mathrm{T}} : \sigma_p \,\mathrm{d}S - \int_V \delta\mathbf{u}^{\mathrm{T}} \cdot \mathbf{b} \,\mathrm{d}V - \int_{S_\sigma} \delta\mathbf{u}^{\mathrm{T}} \cdot \bar{\mathbf{t}} \,\mathrm{d}S - \delta \int_{S_u} (\tilde{\mathbf{u}} - \bar{\mathbf{u}})^{\mathrm{T}} \cdot \alpha \cdot (\tilde{\mathbf{u}} - \bar{\mathbf{u}}) \,\mathrm{d}S = 0, \quad (26)$$

where σ_p is the pseudo-stress, ε_p is the pseudo-strain, $\mathbf{b}$ is a body force vector, and α is a diagonal matrix of penalty coefficients which are usually very large numbers.

For free vibration analysis of thin plates, in order to produce a positive-definite stiffness matrix with smallest dimension for the eigenvalue equation in computing natural frequencies, the discrete system equation and the boundary condition equation are formulated separately. The variational form of the elastic dynamical undamped equilibrium equation can still be taken as usual form as follows:

$$\int_S \delta\varepsilon_p^{\mathrm{T}} : \sigma_p \,\mathrm{d}S + \int_V \delta\mathbf{u}^{\mathrm{T}} \cdot \rho\ddot{\mathbf{u}} \,\mathrm{d}V - \int_V \delta\mathbf{u}^{\mathrm{T}} \cdot \mathbf{b} \,\mathrm{d}V - \int_{S_\sigma} \delta\mathbf{u}^{\mathrm{T}} \cdot \bar{\mathbf{t}} \,\mathrm{d}S = 0, \quad (27)$$

where $\mathbf{b}$ is a body force vector and ρ is the mass density.

The weak form of the essential boundary conditions with Lagrange multipliers is employed to produce the discretized essential boundary conditions as given below

$$\int_{S_u} \delta\lambda^{\mathrm{T}} (\tilde{\mathbf{u}} - \bar{\mathbf{u}}) \,\mathrm{d}S = 0. \quad (28)$$

The Lagrange multipliers λ can be written as follows:

$$\lambda(\mathbf{X}) = N_I(s)\lambda_I, \quad \mathbf{X} \in S_u, \quad (29)$$

$$\delta\lambda(\mathbf{X}) = N_I(s)\delta\lambda_I, \quad \mathbf{X} \in S_u, \quad (30)$$

where s and $N_I(s)$ are the arclength and Lagrange interpolation along the boundary respectively.

The displacement fields of a Kirchhoff plate [22] are

$$\mathbf{u} = \begin{Bmatrix} u \\ v \\ w \end{Bmatrix} = \begin{Bmatrix} -z\dfrac{\partial}{\partial x} & -z\dfrac{\partial}{\partial y} & 1 \end{Bmatrix}^{\mathrm{T}} \quad w = \tilde{\mathbf{L}}w. \tag{31}$$

The pseudo-strains of the plate are denoted as

$$\varepsilon_p = \begin{Bmatrix} -\dfrac{\partial^2}{\partial x^2} & -\dfrac{\partial^2}{\partial y^2} & -2\dfrac{\partial^2}{\partial x\,\partial y} \end{Bmatrix}^{\mathrm{T}} \quad w = \mathbf{L}w. \tag{32}$$

The pseudo-stresses or moments (per unit length) of the plate are denoted as

$$\sigma_p = \begin{Bmatrix} M_x \\ M_y \\ M_{xy} \end{Bmatrix}. \tag{33}$$

The relationship between the strain and the stress is expressed as

$$\sigma_p = D\mathbf{C}\varepsilon_p, \tag{34}$$

where $D = Eh^3/12(1-v^2)$, and with E and v being Young's modulus, and the Poisson ratio respectively, and

$$\mathbf{C} = \begin{bmatrix} 1 & v & 0 \\ v & 1 & 0 \\ 0 & 0 & \frac{1}{2}(1-v) \end{bmatrix},$$

The static variational form (26) can be rewritten as

$$\int_S \delta w \mathbf{L}^{\mathrm{T}} D\mathbf{C}\mathbf{L}w\,\mathrm{d}S - \int_V \delta w \tilde{\mathbf{L}}^{\mathrm{T}}\mathbf{b}\,\mathrm{d}V - \int_{S_\sigma} \delta w \tilde{\mathbf{L}}^{\mathrm{T}}\bar{\mathbf{t}}\,\mathrm{d}S - \delta\int_{S_u} (\mathbf{R}w - \bar{\mathbf{u}})^{\mathrm{T}}\alpha(\mathbf{R}w - \bar{\mathbf{u}})\,\mathrm{d}S = 0. \tag{35}$$

The dynamical variational form (27) can be rewritten as

$$\int_S \delta w \mathbf{L}^{\mathrm{T}} D\mathbf{C}\mathbf{L}w\,\mathrm{d}S + \int_V \rho\delta w \tilde{\mathbf{L}}^{\mathrm{T}}\tilde{\mathbf{L}}\ddot{w}\,\mathrm{d}V - \int_V \delta w \tilde{\mathbf{L}}^{\mathrm{T}}\mathbf{b}\,\mathrm{d}V - \int_{S_\sigma} \delta w \tilde{\mathbf{L}}^{\mathrm{T}}\bar{\mathbf{t}}\,\mathrm{d}S = 0. \tag{36}$$

The weak form (28) can be rewritten as

$$\int_{S_u} \delta\lambda^{\mathrm{T}}(\mathbf{R}w - \bar{\mathbf{u}})\,\mathrm{d}S = 0. \tag{37}$$

4. DISCRETE EQUATIONS

Substituting the displacement field w of form (7) into the variational form (35), the final static discrete equation can be obtained as follows:

$$(\mathbf{K} + \tilde{\mathbf{K}})\mathbf{w} = \mathbf{f}. \tag{38}$$

Similarly, substituting the displacement field w of form (7) into the variational form (36), the final dynamical discrete equation can be obtained as follows:

$$\mathbf{M}\ddot{\mathbf{w}} + \mathbf{K}\mathbf{w} = \mathbf{f} \tag{39}$$

and

$$K_{IJ} = \int_S \mathbf{B}_I^{\mathrm{T}} D\mathbf{C}\mathbf{B}_J \,\mathrm{d}S, \qquad \tilde{K}_{IJ} = \int_S \Psi_I^{\mathrm{T}} \beta \Psi_J \,\mathrm{d}S, \tag{40, 41}$$

$$M_{IJ} = \int_S \rho\left(\Phi_I \Phi_J h + \Phi_{I,x}\Phi_{J,x}\frac{h^3}{12} + \Phi_{I,y}\Phi_{J,y}\frac{h^3}{12}\right)\mathrm{d}S, \tag{42}$$

$$f_I = \int_V F_I^{\mathrm{T}} \mathbf{b} \,\mathrm{d}V + \int_{S_\sigma} \mathbf{F}_I^{\mathrm{T}} \bar{\mathbf{t}} \,\mathrm{d}S, \tag{43}$$

$$\mathbf{B}_I = \begin{Bmatrix} -\Phi_{I,xx} \\ -\Phi_{I,yy} \\ -2\Phi_{I,xy} \end{Bmatrix}, \qquad \mathbf{F}_I = \begin{Bmatrix} -z\Phi_{I,x} \\ -z\Phi_{I,y} \\ \Phi_I \end{Bmatrix}. \tag{44, 45}$$

For clamped boundary,

$$\Psi_I = \begin{Bmatrix} \Phi_I \\ \Phi_{I,n} \end{Bmatrix}.$$

For simply supported boundary,

$$\Psi_I = \begin{Bmatrix} \Phi_I \\ \Phi_{I,nn} \end{Bmatrix},$$

where n is the unit normal to the essential boundary surfaces S_u.

5. EIGENVALUE PROBLEM

5.1. ESSENTIAL BOUNDARY CONDITION

Substituting the displacement field w of form (7) into the weak form (37), yields a set of linear algebraic constraint equations:

$$\mathbf{H}\mathbf{w} = \mathbf{q} \quad \text{and} \quad \mathbf{H}_{KI} = \int_{S_u} \mathbf{N}_K \Psi_I \,\mathrm{d}S \tag{46, 47}$$

$$\mathbf{q}_K = \int_{S_u} \mathbf{N}_K \bar{\mathbf{u}}\, \mathrm{d}S, \qquad \mathbf{N}_K = \begin{bmatrix} N_K & 0 \\ 0 & N_K \end{bmatrix}, \tag{48, 49}$$

$$\mathbf{w} = \{w_1, \ldots, w_n\}^{\mathrm{T}}, \tag{50}$$

where n is the total number of nodes in the domain V. In general, $\mathbf{H}$ is a singular matrix.

For clamped boundary,

$$\Psi_I = \begin{Bmatrix} \Phi_I \\ \Phi_{I,n} \end{Bmatrix}.$$

For simply supported boundary,

$$\Psi_I = \begin{Bmatrix} \Phi_I \\ \Phi_{I,nn} \end{Bmatrix},$$

where n is the unit normal to the essential boundary surface S_u.

5.2. EIGENVALUE EQUATION

Eigenvalue equation of plate conducted from equation (39) is given by

$$(\mathbf{K} - \omega^2 \mathbf{M})\mathbf{Q} = 0, \tag{51}$$

where ω is the circular frequency, and $\mathbf{Q}$ is a matrix of eigenvectors given by

$$\mathbf{Q} = \{Q_1, \ldots, Q_n\}^{\mathrm{T}}. \tag{52}$$

For all the eigenvectors, the boundary constraint equation (46) can be restated as

$$\mathbf{HQ} = \mathbf{q}. \tag{53}$$

For eigenvalue analysis, the essential boundary conditions are homogeneous, therefore, we have $\mathbf{q} = 0$. Using singular-value decomposition [23], $\mathbf{H}$ can be decomposed as

$$\mathbf{H} = \mathbf{U}\Sigma\mathbf{V}^{\mathrm{T}}, \tag{54}$$

where $\mathbf{U}$ and $\mathbf{V}$ are orthogonal matrices, Σ has a diagonal form whose diagonal elements are equal to singular values of $\mathbf{H}$.

The matrix $\mathbf{V}$ can be written as

$$\mathbf{V}^{\mathrm{T}} = \{\mathbf{V}_{n\times r}, \mathbf{V}_{n\times(n-r)}\}^{\mathrm{T}}, \tag{55}$$

where r is the rank of $\mathbf{H}$, namely the number of independent constraints.

Performing co-ordinate transformation

$$\mathbf{Q} = \mathbf{V}_{n\times(n-r)}\tilde{\mathbf{Q}} \tag{56}$$

and substituting equation (56) into equation (51), leads to

$$(\tilde{\mathbf{K}} - \omega^2 \tilde{\mathbf{M}})\tilde{\mathbf{Q}} = 0, \tag{57}$$

where $\tilde{\mathbf{K}} = \mathbf{V}^{\mathrm{T}}_{(n-r)\times n}\mathbf{K}\mathbf{V}_{n\times(n-r)}$ and $\tilde{\mathbf{M}} = \mathbf{V}^{\mathrm{T}}_{(n-r)\times n}\mathbf{M}\mathbf{V}_{n\times(n-r)}$ are the dimension reduced stiffness and mass matrices, which are non-negative definite. Solving equation (57) gives natural frequencies of the vibration of plates.

6. NUMERICAL EXAMPLES

6.1. STATIC DEFLECTION OF BENDING THIN PLATES

For static deflection analysis of bending thin plates shown in Figure 1, the following parameters are used: length in x direction $a = 0{\cdot}6$ m for rectangular plate; length $a = b = 0{\cdot}6$ m for square plate; thickness $h = 0{\cdot}001$ m; Young's modulus $E = 1{\cdot}0 \times 10^9$ N/m^2; and the Poisson ratio $v = 0{\cdot}3$.

For static problem, a concentrated force at the center of the plates $P = 100{\cdot}0$ N.

Dimensionless deflection coefficient β of center of thin rectangular plate is defined as $\beta = w_{max}D/Pa^2$, where w_{max} is the deflection at the center of the plates and $D = Eh^3/[12(1-v^2)]$ is the flexural rigidity of the plates.

In order to analyze the convergence of the present method, we calculated deflections of a square plate using different density of nodes. Two kinds of boundary conditions are imposed: simply supported and fully clamped. The results are shown in Table 1 together with analytical results. Good convergence has been achieved.

Further examinations are performed for different aspect ratios. The deflections are calculated using 16×16 nodes in the present method. The results are shown in Tables 2 and 3. Compared with Timoshenko's results, good agreements have been achieved for all the cases.

TABLE 1

Deflection of a square plate

	β (present method)					β [22] (Timoshenko)
Nodes	6×6	9×9	12×12	15×15	18×18	
S–S–S–S	0·01032	0·01141	0·01145	0·01155	0·01157	0·01160
C–C–C–C	0·00452	0·00538	0·00546	0·00552	0·00554	0·00560

TABLE 2

Deflection of simply supported rectangular plates

b/a	1·0	1·2	1·4	1·6	1·8	2·0
β (present method)	0·01157	0·01344	0·01476	0·01556	0·01603	0·01632
β [22] (Timoshenko)	0·01160	0·01353	0·01484	0·01570	0·01620	0·01651

TABLE 3

Deflection of fully clamped rectangular plates

b/a	1·0	1·2	1·4	1·6	1·8	2·0
β (present method)	0·00552	0·00637	0·00680	0·00698	0·00703	0·00704
β [22] (Timoshenko)	0·00560	0·00647	0·00691	0·00712	0·00720	0·00722

6.2. FREQUENCY ANALYSIS OF FREE VIBRATION OF THIN PLATES

Consider now a square plate with the following parameters: length $a = b = 10{\cdot}0$ m; thickness $h = 0{\cdot}05$ m; Young's modulus $E = 200 \times 10^9$ N/m^2; the Poisson ratio $\nu = 0{\cdot}3$; and mass density $\rho = 8000$ Kg/m^3.

An elliptical plate was studied. The radii of the plate are $a = 5{\cdot}0$ m and $b = 2{\cdot}5$ m respectively. Other parameters are the same as the square plate.

A hexagonal plate was studied. The length of each side is $a = 10{\cdot}0$ m. Other parameters are the same as the square plate.

A plate of very complicated shape was also studied. The geometric parameters are shown in Figure 8. The unit is meter. Other parameters are the same as the square plate.

Different boundary conditions were considered to examine the present method in imposing boundary conditions.

The frequency coefficients in the tables are $\Omega_1 = (\omega^2 \rho h a^4/D)^{1/4}$, $\Omega_2 = (\omega^2 \rho h a_p^4/D)^{1/4}$, where a_p is the radius of the inscribing circle for regular polygonal plates.

6.2.1. *Free thin square plate*

We calculated frequencies of free vibration of free thin square plate. The results using regular nodes of different density are shown in Table 4 together with FEM results. In the FEM results, HOE denotes eight-noded semi-loof thin shell element (4×4 mesh); LOE denotes four-noded iso-parametric shell element (8×8 mesh). The first three frequencies corresponding to the rigid displacements are zero, and are not listed in the table. The results obtained using the present method are between those of FEMs using HOE and LOE. The present results show good convergence and good agreements with other methods.

6.2.2. *Simply supported and fully clamped thin square plate*

Natural frequencies of lateral free vibration of a simply supported and fully clamped thin square plate are computed using the present method. In order to analyze the effectiveness of the present method using irregular nodes, we calculated frequencies using 13×13 regular nodes (Figure 2) and 169 irregular nodes (Figure 3). The results are shown in Tables 5 and 6. It is found that the results of using both regular and irregular nodes show good agreements with each other and with the analytical solutions.

6.2.3. *Thin elliptical plate*

In order to analyze the effectiveness of the present method in computing frequencies of free vibration of thin plate of complicated shape, we calculated natural frequencies of a thin

TABLE 4

Natural frequency coefficients Ω_1 of lateral free vibration of a free square plate

Mode	Analytical solution [24]	Present method				FEM [24]	
		5×5	9×9	13×13	17×17	HOE	LOE
4	3·670	3·700	3·670	3·670	3·670	3·567	3·682
5	4·427	4·468	4·434	4·430	4·429	4·423	4·466
6	4·926	5·000	4·939	4·933	4·930	4·875	4·997
7	5·929	6·010	5·907	5·903	5·901	5·851	5·942
8	5·929	6·010	5·907	5·903	5·901	5·851	5·942
9	7·848	8·189	7·855	7·840	7·832	7·820	8·079

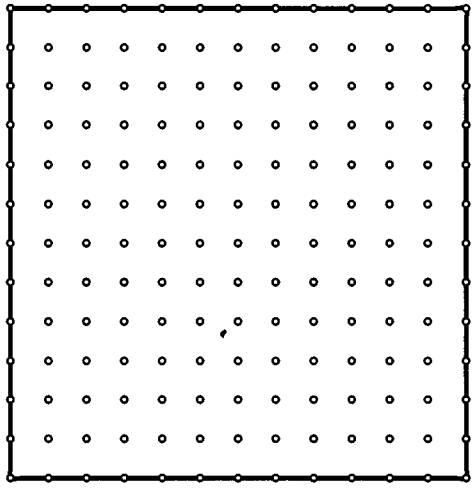

Figure 2. A square plate with 13×13 regular nodes.

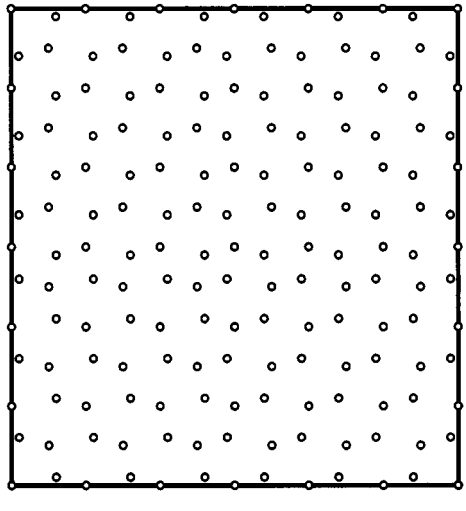

Figure 3. A square plate with 169 irregular nodes.

elliptical plate. Table 7 shows frequencies of a free thin elliptical plate using regular nodes. The first three frequencies corresponding to rigid displacements are zero, and are not listed in the table. Good convergence of the results has been achieved. Table 8 shows frequencies of fully clamped thin elliptical plate. The frequencies are calculated using regular nodes (Figure 4) and irregular nodes (Figure 5). Good agreement between the same using regular and irregular nodes has been observed.

6.2.4. *Fully clamped thin regular polygonal plates*

The natural frequencies of a square plate with fully clamped boundaries were calculated. A total of 524 irregular nodes shown in Figure 6 were used. The natural frequencies of a hexagonal plate with fully clamped boundaries were also calculated, where 380 irregular

TABLE 5

Natural frequency coefficients Ω_1 of lateral free vibration of a simply supported square plate

Mode	Analytical solution [24]	Present method	
		Regular nodes 13×13	Irregular nodes 169
1	4·443	4·443	4·453
2	7·025	7·031	7·033
3	7·025	7·036	7·120
4	8·886	8·892	8·912
5	9·935	9·959	9·966
6	9·935	9·966	10·010
7	11·327	11·341	11·345
8	11·327	11·347	11·540
9	—	13·032	12·994
10	—	13·036	13·064

TABLE 6

Natural frequency coefficients Ω_1 of lateral free vibration of a fully clamped square plate

Mode	Analytical solution [25]	Present method	
		Regular nodes 13×13	Irregular nodes 169
1	5·999	6·017	5·999
2	8·568	8·606	8·596
3	8·568	8·606	8·602
4	10·407	10·439	10·421
5	11·472	11·533	11·507
6	11·498	11·562	11·528
7	—	12·893	12·925
8	—	12·896	12·986
9	—	14·605	14·570
10	—	14·606	14·604

TABLE 7

Natural frequency coefficients Ω_1 of lateral free vibration of a free elliptical plate

Mode	Present method		
	97 nodes	241 nodes	289 nodes
4	5·197	5·176	5·173
5	6·533	6·509	6·505
6	8·288	8·244	8·234
7	9·451	9·405	9·397
8	10·602	10·559	10·547
9	11·333	11·256	11·249
10	12·223	12·168	12·160

TABLE 8

Natural frequency coefficients Ω_1 of lateral free vibration of a fully clamped elliptical plate

Mode	Present method	
	Regular nodes 201	Irregular nodes 201
1	10·467	10·454
2	12·619	12·621
3	15·009	14·992
4	16.726	16.716
5	17·629	17·658
6	18·838	18·840
7	20·604	20·508
8	21·081	21·060
9	22·913	22·890
10	23·610	23·591

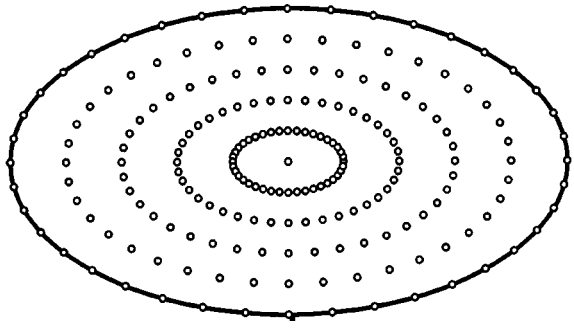

Figure 4. An elliptical plate with 201 regular nodes.

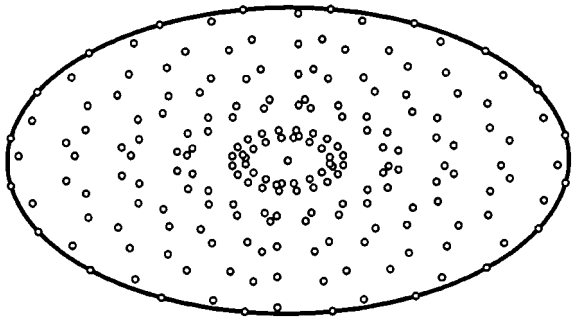

Figure 5. An elliptical plate with 201 irregular nodes.

nodes shown in Figure 7 were used. Table 9 lists the frequency coefficients of the lowest 10 modes for these two plates. Table 10 shows a comparison between the frequency coefficients using the EFG method and those given by reference [26]. For the square plate, the natural frequency coefficient of the first mode using the EFG method agrees very well with the exact solution and the numerical result in reference [26]. For the hexagonal plate, the natural

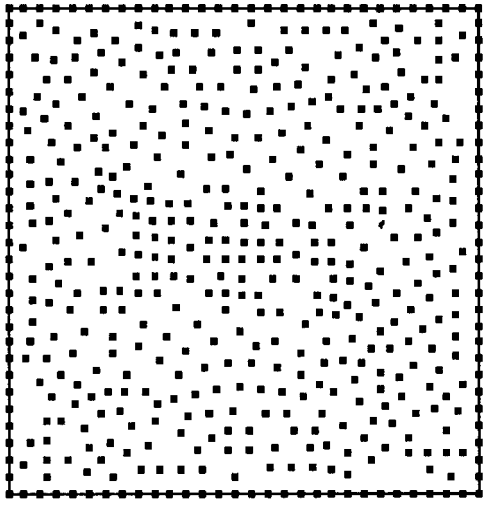

Figure 6. A square plate with 524 irregular nodes.

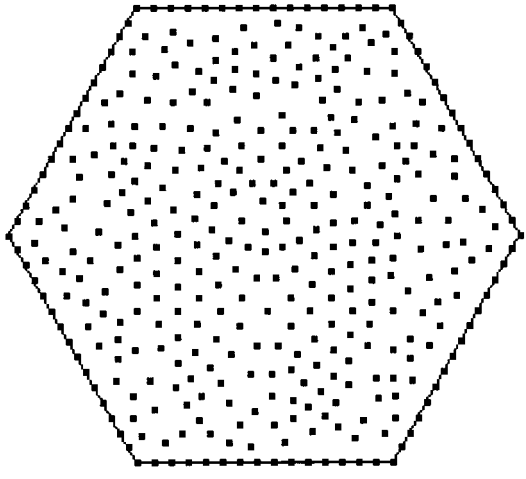

Figure 7. A hexagonal plate with 380 irregular nodes.

frequency coefficient of the first mode using the EFG method is slightly smaller than the numerical result in reference [26].

6.2.5. *Thin plate of complicated shape*

The natural frequencies are computed for a thin plate with a hole of very complicated shape shown in Figure 8. The plate is chosen highly hypothetically, but it serves the purpose of demonstrating the applicability of the present method to plates of complicated shapes. The nodal distribution is plotted in Figure 9. Table 11 lists the frequencies obtained for the plate with different boundary conditions. In the table, S denotes simply supported while C means clamped. As expected, the natural frequencies of the plate with clamped boundaries are generally higher than those with simply supported boundaries.

TABLE 9

Natural frequency coefficients Ω_2 of lateral free vibration of fully clamped regular polygonal plate

Mode	Present method	
	Square	Hexagon
1	9·089	9·042
2	18·700	17·805
3	18·829	20·586
4	28·121	29·802
5	33·515	34·740
6	33·649	37·368
7	42·550	46·622
8	43·529	51·846
9	53·896	55·799
10	54·156	59·138

TABLE 10

Comparison of natural frequency coefficients Ω_2 of first mode of fully clamped regular polygonal plates

	Present method	Exact [26]	Ref. [26]
Square	9·089	8·997	9·122
Hexagon	9·042	—	9·638

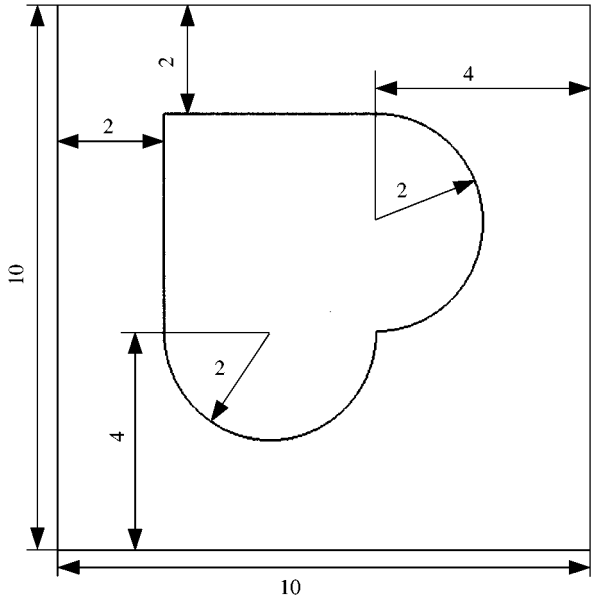

Figure 8. A plate with a hole of complicated shape.

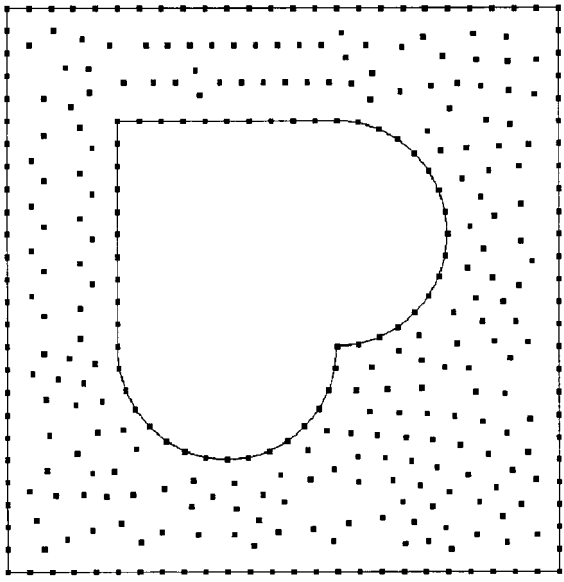

Figure 9. Nodal distribution in a plate with a hole of complicated shape.

TABLE 11

Natural frequency coefficients Ω_1 of lateral free vibration of a plate with a hole of complicated shape

Mode	Present method			
	S–S–S–S	C–C–C–C	S–C–S–C	S–C–C–S
1	5·453	7·548	7·170	6·079
2	8·069	10·764	10·343	9·204
3	9·554	11·113	11·415	10·837
4	10·099	11·328	12·572	11·273
5	11·328	12·862	12·811	12·278
6	12·765	13·300	13·272	13·322
7	13·685	14·168	13·997	14·308
8	14·305	15·369	14·627	14·900
9	15·721	16·205	15·743	15·170
10	17·079	17·137	16·391	16·302

7. CONCLUSIONS

A mesh-free method has been developed for static and free vibration analyses of thin plates of complicated shapes. The present method does not require a mesh for displacement field interpolation. Numerical examples are presented for plates of different shapes with irregular node distribution. Very good convergence of the present method has been observed. Very good agreements with analytical results as well as FEM have also been achieved. It has been demonstrated that the present method is efficient in performing static and free vibration analyses of thin plates of complicated shapes.

REFERENCES

1. J. DOLBOW and T. BELYTSCHKO 1998 *Archives of Computational Methods in Engineering* **5**, 207–241. An introduction to programming the meshless element free Galerkin method.
2. W. K. LIU, S. JUN, S. F. LI, J. ADEE and T. BELYTSCHKO 1995 *International Journal for Numerical Methods in Engineering* **38**, 1655–1679. Reproducing kernel particle methods for structural dynamics.
3. G. R. LIU, K. Y. YANG and M. CHENG 1999 *Fourth International Asia–Pacific Conference on Computational Mechanics*, *Singapore*. Some recent development in element free methods in computational mechanics.
4. B. M. DONNING and W. K. LIU 1998 *Computer Methods in Applied Mechanics and Engineering* **152**, 47–71. Meshless methods for shear-deformable beams and plates.
5. G. R. LIU 1999 *Impact Response of Materials and Structures* (V. P. W. Shim et al., editors) 475–480 Oxford: University Press. A point assembly method for stress analysis for solid.
6. G. R. LIU and Y. T. GU 2001 *International Journal for Numerical Methods in Engineering* **50**, 937–951. A point interpolation method for two-dimensional solids.
7. Y. T. GU and G. R. LIU 2001 *Computational Mechanics.* A boundary point interpolation method for stress analysis of solids (in press).
8. G. R. LIU and K. Y. YANG 1999 *Fourth International Asia–Pacific Conference on Computational Mechanics*, *Singapore*. A new meshless method for stress analysis for solids and structures.
9. M. CHENG and G. R. LIU 1999 *Fourth International Asia–Pacific Conference on Computational Mechanics*, *Singapore*. A finite point method for analysis of fluid flow.
10. X. G. XU and G. R. LIU 1999 *Fourth International Asia–Pacific Conference on Computational Mechanics*, *Singapore*. A local-function approximation method for simulating two-dimensional incompressible flow.
11. B. NAYROLES, G. TOUZOT and P. VILLON 1992 *Computational Mechanics* **10**, 307–318. Generalizing the finite element method: diffuse approximation and diffuse elements.
12. T. BELYTSCHKO, P. KRYSL and Y. KRONGAUZ 1997 *International Journal for Numerical Methods in Fluids* **24**, 1253–1270. A three-dimensional explicit element-free Galerkin method.
13. T. BELYTSCHKO, Y. Y. LU and L. GU 1995 *Engineering and Fracture Mechanics* **32**, 2547–2570. Crack propagation by element-free Galerkin methods.
14. P. KRYSL and T. BELYTSCHKO 1995 *Computational Mechanics,* **17**, 26–35. Analysis of thin plates by the element-free Galerkin method.
15. P. KRYSL and T. BELYTSCHKO 1996 *International Journal of Solids and Structures* **33**, 3057–3080. Analysis of thin shells by the element-free Galerkin method.
16. A. E. OUATOUATI and D. A. JOHNSON 1999 *International Journal for Numerical Methods in Engineering* **46**, 1–27. A new approach for numerical modal analysis using the element-free method.
17. G. R. LIU and K. Y. YANG 1998 *The Proceedings of the Third HPC Asia'98*, *Singapore*, 715–721. A penalty method for enforcing essential boundary conditions in element free Galerkin method.
18. D. HEGEN 1996 *Computer Methods in Applied Mechanics and Engineering* **135**, 143–166. Element-free Galerkin methods in combination with finite element approaches.
19. Y. T. GU and G. R. LIU 2001 *Computer Methods in Applied Mechanics and Engineering*. A coupled element Galerkin/boundary element method for stress analysis of two-dimension (In press).
20. G. R. LIU and Y. T. GU 2000 *Computational Mechanics* **26**, 166–173. Coupling element free Galerkin and hybrid boundary element methods using modified variational formulation.
21. G. R. LIU and L. YAN 1999 *Fourth International Asia–Pacific Conference on Computational Mechanics*, *Singapore*. A study on numerical integration in element-free Galerkin method.
22. S. P. TIMOSHENKO and S. WOINOWSKY-KRIEGER 1995 *Theory of Plates and Shells*. New York: McGraw-Hill; second edition.
23. D. H. GRIFFEL 1989 *Linear Algebra and its Applications*. New York: Ellis Horwood Limited.
24. F. ABBASSIAN, D. J. DAWSWELL and N. C. KNOWLES 1987 *Free Vibration Benchmarks*. Atkins Engineering Sciences: Glasgow.
25. D. B. ROBERT 1979 *Formulas for Natural Frequency and Mode Shape*. New York: Van Nostrand Reinhold Company.
26. R. SCHINZINGER and P. A. A. LAURA 1991 *Conformal Mapping Methods and Applications*. New York: Elsevier Science Publishing Company Inc.